

AD-A139 051

THE BEAM-DENSITY EFFECT ON ENERGY LOSS OF A
RELATIVISTIC CHARGED PARTICLE BEAM(U) NAVAL SURFACE
WEAPONS CENTER SILVER SPRING MD D W RULE SEP 83

1/1

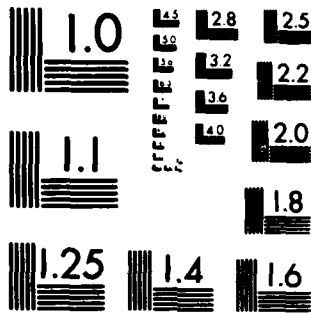
UNCLASSIFIED

NSWC/TR-83-348

F/G 20/8

NL

END
DATE
FILMED
4-84
DTIC



MICROCOPY RESOLUTION TEST CHART
NATIONAL BUREAU OF STANDARDS-1963-A

12

NSWC TR 83-348

THE BEAM-DENSITY EFFECT ON ENERGY LOSS OF A RELATIVISTIC CHARGED PARTICLE BEAM

BY D. W. RULE

RESEARCH AND TECHNOLOGY DEPARTMENT

SEPTEMBER 1983

Approved for public release, distribution unlimited.

AD A139051

DTIC
ELECTE
MAR 16 1984
S E D

FILE COPY



NAVAL SURFACE WEAPONS CENTER

Deligon, Virginia 22448 • Silver Spring, Maryland 20910

84 08 15 004

UNCLASSIFIED

SECURITY CLASSIFICATION OF THIS PAGE (When Data Entered)

REPORT DOCUMENTATION PAGE		READ INSTRUCTIONS BEFORE COMPLETING FORM
1. REPORT NUMBER NSWC TR 83-348	2. GOVT ACCESSION NO. AD-A139051	3. RECIPIENT'S CATALOG NUMBER
4. TITLE (and Subtitle) THE BEAM-DENSITY EFFECT ON ENERGY LOSS OF A RELATIVISTIC CHARGED PARTICLE BEAM	5. TYPE OF REPORT & PERIOD COVERED Final, Fiscal year 83	
	6. PERFORMING ORG. REPORT NUMBER	
7. AUTHOR(s) D. W. Rule	8. CONTRACT OR GRANT NUMBER(s)	
9. PERFORMING ORGANIZATION NAME AND ADDRESS Naval Surface Weapons Center (Code R41) White Oak Silver Spring, MD 20910	10. PROGRAM ELEMENT, PROJECT, TASK AREA & WORK UNIT NUMBERS 62768N R40BJ F68343 SF68343001	
11. CONTROLLING OFFICE NAME AND ADDRESS	12. REPORT DATE September 1983	
	13. NUMBER OF PAGES 39	
14. MONITORING AGENCY NAME & ADDRESS (if different from Controlling Office)	15. SECURITY CLASS. (of this report) UNCLASSIFIED	
	15a. DECLASSIFICATION/DOWNGRADING SCHEDULE	
16. DISTRIBUTION STATEMENT (of this Report) Approved for public release, distribution unlimited.		
17. DISTRIBUTION STATEMENT (of the abstract entered in Block 20, if different from Report)		
18. SUPPLEMENTARY NOTES		
19. KEY WORDS (Continue on reverse side if necessary and identify by block number) Charged particle beams Beam-density effect Energy Loss Energy deposition		
20. ABSTRACT (Continue on reverse side if necessary and identify by block number) Starting from the expression for the cooperative ionization energy loss by a pair of relativistic particles, a formula is derived for the beam-density effect on ionization energy loss for a finite length beam with a Gaussian radial profile. As an example, this formula is evaluated for a 50 MeV, 10 KA electron pulse of one meter length interacting with weakly ionized nitrogen. In this case a large beam-density effect on energy loss was obtained and its dependence on the ionization state of the medium was		

UNCLASSIFIED

SECURITY CLASSIFICATION OF THIS PAGE (When Data Entered)

demonstrated. The relationship of this formulation of energy loss with previous single-particle and beam-plasma loss concepts is discussed.

UNCLASSIFIED

SECURITY CLASSIFICATION OF THIS PAGE(When Data Entered)

FOREWORD

Starting from the expression for the cooperative ionization energy loss by a pair of relativistic particles, a formula is derived for the beam-density effect on ionization energy loss for a finite length beam with a Gaussian radial profile. As an example, this formula is evaluated for a 50 MeV, 10 KA electron pulse of one meter length interacting with weakly ionized nitrogen. In this case a large beam-density effect on energy loss was obtained and its dependence on the ionization state of the medium was demonstrated. The relationship of this formulation of energy loss with previous single-particle and beam-plasma loss concepts is discussed.

This work was supported by the Directed Energy Program Office of the Naval Sea Systems Command and by the Naval Surface Weapons Center's Independent Research Program.

Approved by:

Ira M. Blatstein
 IRA M. BLATSTEIN, Head
 Radiation Division



Accession For	
NTIS GRA&I	<input checked="" type="checkbox"/>
DTIC TAB	<input type="checkbox"/>
Unannounced	<input type="checkbox"/>
Justification	
By _____	
Distribution/	
Availability Codes	
Dist	Special
A-1	

CONTENTS

<u>Chapter</u>		<u>Page</u>
1	INTRODUCTION	1
2	CALCULATION OF THE BEAM-DENSITY EFFECT FOR A FINITE BEAM PULSE	3
	THE INTEGRATION OVER THE BEAM DISTRIBUTION FUNCTION . .	3
	THE FREQUENCY INTEGRATION	7
3	NUMERICAL RESULTS FOR A RELATIVISTIC BEAM	15
4	DISCUSSION	23
	REFERENCES	27

ILLUSTRATIONS

<u>Figure</u>		<u>Page</u>
1	THE CONTOURS IN THE COMPLEX FREQUENCY PLANE USED TO EVALUATE $I(C_+)$ AND $I(C_-)$, EQUATIONS (2.20) and (2.21) . .	10
2	THE RATIO OF THE BEAM-DENSITY ENERGY LOSS TO THE SINGLE PARTICLE ENERGY LOSS, W_B/S	19

TABLES

<u>Table</u>		<u>Page</u>
1	INPUT PARAMETERS TO CHARACTERIZE THE N_2 MEDIUM	16

CHAPTER 1

INTRODUCTION

The application of charged particle beam drivers to inertial confinement fusion has spurred interest in the study of energy deposition by intense beams in extreme states of matter. Enhancement of energy deposition by beams has been predicted on the basis of various modifications of single-particle energy deposition theory, for example: collective beam-target interactions, finite target temperature effects, and beam stagnation in the target. A review of these topics has been given by Toepfer.¹ Observations by Imasaki et al.^{2,3} have shown that enhanced deposition by electrons occurs in thin targets and that there is a strong dependence of the effect on target material. They have suggested that the observations are explained by the collective interaction of the beam with the target. Recently an experiment and calculation by Young et al.⁴ have demonstrated enhanced energy deposition by a deuteron beam in thin targets. The calculation indicates that the enhancement is caused by the free target electrons which are ionized by the early part of the beam pulse. Another example of increased energy deposition is the observation by Kiselev et al.⁵ of the range shortening for a 2 MeV, 1A beam in air. They proposed that a collective interaction of the beam with the plasma that it generates could explain this result.

McCorkle and Iafrate⁶ have suggested that single-particle energy deposition theory should be augmented with a beam-density term when intense beams interact with a plasma. The beam-density effect has its origin in the theory of stopping power of molecular ion clusters, given by Brandt, Rathowski, and Ritchie,⁷⁻⁹ which is in turn closely connected with wakes induced in the conduction electrons of solids.¹⁰⁻¹² McCorkle and Iafrate⁶ modified the nonrelativistic molecular cluster theory⁷ so that it contained a characteristic relativistic screening length and used the result to estimate the beam-density contribution to energy loss by relativistic beams in a plasma. They found that the effect could be quite large relative to single-particle energy loss. McCorkle and Cox¹³ have investigated the relationship between these beam concepts and ohmic loss and return currents.¹⁴⁻¹⁸

A detailed derivation of energy loss by clusters of relativistic particles has been given by Rule and Cha,¹⁹ which includes the Fermi density effect,²⁰ and which reduces to the nonrelativistic theory in the appropriate limit. Recently Rule and Crawford²¹ have shown that the nonrelativistic energy loss expression for a cluster contains long-range dipole-like terms and that this results in a beam-density effect which depends on the beam shape in an essential way.

The present paper contains a detailed theory of the beam-density effect for finite relativistic beams, starting from the results of Reference 19. An example based on this theory is given for a 50 MeV, 10 KA pulse of electrons interacting with weakly ionized nitrogen. It is shown that the beam-density effect results in a large enhancement of energy loss for the regime of beam and medium parameters studied. Finally a brief discussion of the relationship of this effect to other related phenomena is given.

CHAPTER 2

CALCULATION OF THE BEAM-DENSITY EFFECT FOR A FINITE BEAM PULSE

THE INTEGRATION OVER THE BEAM DISTRIBUTION FUNCTION

In Reference 19 a general formula for the coherent, cooperative energy loss by a relativistic pair of particles was derived. The case of \vec{v}_i parallel to \vec{v}_j , but $v_i \neq v_j$ was given, where v_i and v_j are the velocities of the particles. For the special case in which $\vec{v}_i = \vec{v}_j = \vec{v}$, a simpler result was obtained (see Equation (3.33) of Reference 19), namely

$$W(z,b) = \frac{4}{\pi} Z_i Z_j e^2 \left(\frac{\omega}{v} \right)^2 \operatorname{Re} \int_0^{\infty} i dv v \cos \left(\frac{\omega}{v} \frac{z v}{v} \right) \frac{1}{\epsilon(v)} (1 - \beta^2 \epsilon(v))$$

$$\times \left\{ \begin{array}{ll} K_0 \frac{b \omega}{v} (1 - \beta^2 \epsilon)^{1/2} & b \geq a \\ K_0 \frac{a \omega}{v} (1 - \beta^2 \epsilon)^{1/2} & b < a \end{array} \right\}. \quad (2.1)$$

The quantities $Z_i e$ and $Z_j e$ are the charges of the particles; $\omega_p^2 = 4\pi n e^2 / m$, where n is the total number of medium electrons per unit volume, both bound and free, and m is the electron's mass; v is the frequency in units of ω_p ; $\epsilon(v)$ is the dielectric function of the medium; and $\beta = v/c$. The coordinates z and b are the magnitudes of the components of the vector \vec{R}_{ij} from particle i to particle j , such that z is parallel to \vec{v} and b is perpendicular to \vec{v} . The

quantity "a" in (2.1) is the minimum impact parameter which may be suitably chosen to take into account, to a good approximation, the close collision portion of the energy loss.¹⁹ The modified Bessel function $K_0(Z)$ appears in (2.1). For the special case of particles traveling in a line parallel to \vec{v} , an analytic expression for (2.1) has been obtained.²⁰

The limiting case in which $z \rightarrow 0$ and $b \rightarrow 0$ in (2.1) gives

$$W(0,0) = 2 Z_i Z_j S, \quad (2.2)$$

where

$$S \equiv \frac{2}{\pi} e^2 \left(\frac{\omega_p}{v} \right)^2 \operatorname{Re} \int_0^\infty idv v \left(\frac{1}{\epsilon(v)} - \beta^2 \right) K_0 \left(\frac{\omega_p v}{v} (1 - \beta^2 \epsilon)^{1/2} \right). \quad (2.3)$$

This is the usual expression for the ionization energy loss per unit length of a relativistic particle of unit charge, including the Fermi density effect.²²

Using (2.1) and (2.3), one can write the expression for the total ionization energy loss of a pair of particles separated by the distance R_{ij} as

$$\underline{W}(\vec{R}_{ij}) = Z_i^2 S + Z_j^2 S + W(z, b). \quad (2.4)$$

In the limit $R_{ij} \rightarrow 0$ one obtains, using (2.2),

$$\lim_{R_{ij} \rightarrow 0} \underline{W}(\vec{R}_{ij}) = Z_i^2 S + Z_j^2 S + 2Z_i Z_j S = (Z_i + Z_j)^2 S, \quad (2.5)$$

i.e. the energy loss for a particle of charge $(Z_i + Z_j)e$.

With reference to (2.4), the total energy loss of particle i can be written as

$$\underline{W}_i \equiv Z_i^2 S + \frac{1}{2} W(z, b), \quad (2.6)$$

and similarly for particle j.

If, instead of two particles, a beam of particles is considered then the total energy loss per unit length by the ith particle in the beam can be written, in analogy with (2.6), as

$$\underline{W}_B = Z_i^2 S + W_B, \quad (2.7)$$

where

$$W_B \equiv \frac{1}{2} \int_{-\infty}^{\infty} dz \int_0^{2\pi} d\theta \int_0^{\infty} db b \rho(z, b) W(z, b). \quad (2.8)$$

The factor of 1/2 in (2.6) and in (2.8) avoids double counting of the cooperative terms. The assumption implicit in (2.8) is that, having singled out the ith beam particle, the remainder of the beam is treated as a continuum of charge, i.e. a charged fluid of density $\rho(z, b)$.

In order to proceed further, the form of $\rho(z, b)$ is specified as

$$\rho(z, b) = n_B e^{-\left(\frac{b}{b_0}\right)^2} \theta(z+L_1) \theta(L_2-z) \quad (2.9)$$

Thus a beam having a step function $[\theta(z)]$ head and tail and a Gaussian radial profile will be considered in order to illustrate the properties of the beam-density effect. L_2 is the distance from the particle of interest to the beam's head and L_1 is the distance to the tail. The particle is assumed to be on axis. Setting $Z_i = Z_j$ and using (2.1) and (2.9) in (2.8), W_B becomes

$$W_B = \frac{2e^2}{\pi} \left(\frac{\omega p}{v}\right)^2 n_B \int_{-L_1}^{L_2} dz \int_0^{2\pi} d\theta \int_0^{\infty} db b e^{-\left(\frac{b}{b_0}\right)^2} \operatorname{Re} \int_0^{\infty} idv v \cos\left(\frac{\omega p z v}{v}\right) \frac{1}{\epsilon(v)} \\ \times (1 - \beta^2 \epsilon(v)) K_0\left(\frac{b\omega p}{v} (1 - \beta^2 \epsilon(v))^{1/2}\right). \quad (2.10)$$

Next, the order of the frequency and space integrals is interchanged. This is permissible since the integrand is uniformly convergent for finite z and b . The z -integration yields

$$\int_{-L_1}^{L_2} \cos\left(\frac{\omega p v}{v} z\right) dz = \frac{v}{\omega p v} \left[\sin\left(\frac{\omega p v}{v} L_1\right) + \sin\left(\frac{\omega p v}{v} L_2\right) \right]. \quad (2.11)$$

The b -integration is²³

$$\int_0^{\infty} db b e^{-\left(\frac{b}{b_0}\right)^2} K_0(b/B) = \frac{b_0^2}{4} e^{-(b_0/2B)^2} E_1\left[\left(\frac{b_0}{2B}\right)^2\right], \quad (2.12)$$

where $E_1(z)$ is the exponential integral function, and

$$B^{-1} \equiv \frac{\omega p v}{v} (1 - \beta^2 \epsilon)^{1/2}. \quad (2.13)$$

The correction to the integral for $b < a$, Equation (2.1), has been neglected since it is small. The θ -integration gives a factor of 2π .

Using (2.11)-(2.13) in (2.10), W_B becomes

$$W_B = \frac{n_B b^2}{2} e^{-2} \frac{\omega_p}{v} \operatorname{Re} \int_0^{\infty} dv \frac{1}{\epsilon(v)} (1 - \beta^2 \epsilon(v)) e^{\left(\frac{b}{2} \frac{\omega_p v}{v}\right)^2 (1 - \beta^2 \epsilon)} E_1 \left[\left(\frac{b}{2} \frac{\omega_p v}{v}\right)^2 (1 - \beta^2 \epsilon) \right] \\ \times \begin{bmatrix} e^{\frac{i\omega L v}{v} \frac{p_1}{v}} + e^{\frac{i\omega L v}{v} \frac{p_2}{v}} & -e^{\frac{-i\omega L v}{v} \frac{p_1}{v}} - e^{\frac{-i\omega L v}{v} \frac{p_2}{v}} \end{bmatrix}. \quad (2.14)$$

THE FREQUENCY INTEGRATION

At this point the form of the dielectric function must be specified. The Lorentzian dielectric function of the form

$$\epsilon(v) = 1 + \sum_{i=1}^N \frac{f_i}{v_i^2 - 2in_i v - v^2} \quad (2.15)$$

is chosen. In (2.15), the v_i are the eigenfrequencies of harmonic oscillators which are given values to correspond to atomic transitions, and the n_i are the damping coefficients, or the half widths of the atomic transitions. The oscillator strengths f_i are chosen to equal the fraction of an atom's electrons in a subshell. For conduction electrons $v_j = 0$ and $2n_j$ is the plasmon line width in solids or the collision frequency in a plasma, all in units of ω_p . In short, the parameters in $\epsilon(v)$ are chosen phenomenologically to represent the dielectric properties of various media.

Following the method developed by Sternheimer²⁴ in his calculations of the Fermi density effect,

$$\epsilon^{-1}(\nu) \approx 1 - \sum_{i=1}^N \frac{f_i}{k_i^2 - 2in_i\nu - \nu^2}, \quad (2.16)$$

where $k_i^2 = \rho^2 \nu_i^2 + f_i$. The Sternheimer factor ρ is chosen so that the value of the Bethe logarithm, $\ln I$, obtained in non-relativistic experiments, is reproduced by

$$\sum_{i=1}^N f_i \ln(k_i \hbar \omega_p) = \ln I. \quad (2.17)$$

Defining

$$\alpha_j = -in_j + (k_j^2 - n_j^2)^{1/2}, \quad \beta_j = -in_j - (k_j^2 - n_j^2)^{1/2}, \quad k_j > n_j, \quad (2.18a)$$

and

$$\alpha_j = -i[n_j - (n_j^2 - k_j^2)^{1/2}], \quad \beta_j = -i[n_j + (n_j^2 - k_j^2)^{1/2}], \quad k_j \leq n_j, \quad (2.18b)$$

Equation (2.16) can be rewritten as

$$\epsilon^{-1}(\nu) = 1 + \sum_{j=1}^N \frac{f_j}{(\nu - \alpha_j)(\nu - \beta_j)}; \quad (2.19)$$

therefore $\epsilon^{-1}(\nu)$ has poles at $\nu = \alpha_j$ and $\nu = \beta_j$ in the lower half complex ν -plane.

In order to accomplish the frequency integral of Equation (2.14), two contour integrals will be performed, one in the first quadrant and one in the fourth quadrant of the complex v -plane. Therefore, the following integrals are defined:

$$I(C_+) \equiv \int_{C_+} dv \frac{1}{\epsilon} (1-\beta^2\epsilon) e^{Av^2(1-\beta^2\epsilon)} E_1\left(A v^2(1-\beta^2\epsilon)\right) \left[e^{iB_1 v} + e^{iB_2 v} \right] \quad (2.20)$$

$$I(C_-) \equiv - \int_{C_-} dv \frac{1}{\epsilon} (1-\beta^2\epsilon) e^{Av^2(1-\beta^2\epsilon)} E_1\left(A v^2(1-\beta^2\epsilon)\right) \left[e^{-iB_1 v} + e^{-iB_2 v} \right] \quad (2.21)$$

where

$$A \equiv \left(\frac{b_o \omega}{2v} \right)^2, \quad (2.22)$$

$$B_1 \equiv \frac{\omega L_1}{v} \text{ and } B_2 \equiv \frac{\omega L_2}{v}. \quad (2.23)$$

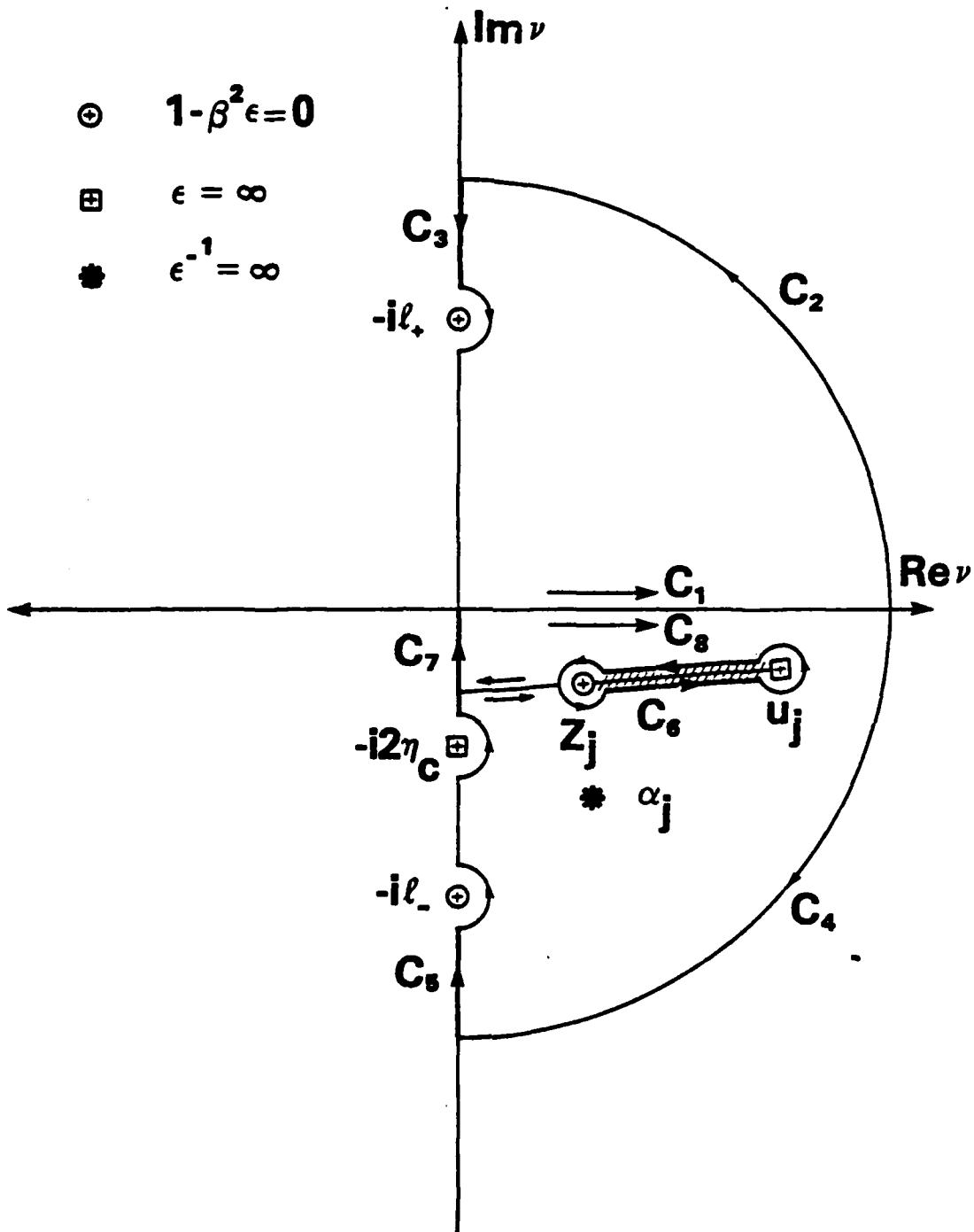
Referring to Figure 1, the integral around the first quadrant is $I(C_+) = 0$ so that

$$I(C_1) = -I(C_3) - I(C_2). \quad (2.24)$$

The integral around the fourth quadrant is $I(C_-) = -2\pi i \sum_{j=1}^N R_j$, where the

R_j are the residues of the poles of $\epsilon^{-1}(v)$. Therefore,

$$I(C_3) = -2\pi i \sum_{j=1}^N R_j - I(C_4) - I(C_5) - I(C_6) - I(C_7). \quad (2.25)$$



⊕ $1 - \beta^2 \epsilon = 0$

⊕ $\epsilon = \infty$

* $\epsilon^{-1} = \infty$

FIGURE 1. THE CONTOURS IN THE COMPLEX FREQUENCY PLANE USED TO EVALUATE I(C₊) AND (C₋), EQUATIONS (2.20) AND (2.21)

Using (2.24) and (2.25) in (2.14), one may write W_B as

$$W_B = \frac{n_B b_0^2}{2} e^2 \frac{\omega}{v} \text{Re} [I(C_1) + I(C_8)]. \quad (2.26)$$

The contour integrals required to evaluate $I(C_1)$ and $I(C_8)$ will be discussed next. As the radii of the quarter circles for C_2 and C_4 become infinite, $I(C_2) \rightarrow 0$ and $I(C_4) \rightarrow 0$. Along C_3 , $v = iy$ and all the factors of the integrand are real except $dv = idy$ and $E_1(Z)$, where

$$Z \equiv Av^2(1 - \beta^2 \epsilon). \quad (2.27)$$

There are zeros of $1 - \beta^2 \epsilon$ on the imaginary axis²⁴, so that

$$1 - \beta^2 \epsilon(+i\underline{l}_+) \equiv 0 \quad (2.28)$$

defines the positions $v = +i\underline{l}_+$ and $v = -i\underline{l}_-$ of the zeroes. Furthermore, one has

$$1 - \beta^2 \epsilon(+iy) > 0 \quad y > \underline{l}_+ \quad (2.29a)$$

and

$$1 - \beta^2 \epsilon(+iy) < 0 \quad y < \underline{l}_+, \quad (2.29b)$$

which gives $Z < 0$ for $y > \underline{l}_+$ and $Z > 0$ for $y < \underline{l}_+$. Hence,

$$E_1(Z) = \begin{cases} -Ei(|Z|) \mp i\pi & , y > \underline{l}_+ \\ E_1(|Z|) & , y < \underline{l}_+ \end{cases} \quad (2.30)$$

Taking (2.30) into account,

$$I(C_3) = -\pi \int_{\ell_+}^{\infty} dy \frac{1}{\epsilon(iy)} \left(1 - \beta^2 \epsilon(iy)\right) e^{-Ay^2(1-\beta^2\epsilon)} [e^{-B_1 y} + e^{-B_2 y}]; \quad (2.31)$$

and similarly

$$I(C_5) = \pi \int_{\ell_-}^{\infty} dy \frac{1}{\epsilon(-iy)} \left(1 - \beta^2 \epsilon(-iy)\right) e^{-Ay^2(1-\beta^2\epsilon)} [e^{-B_1 y} + e^{-B_2 y}]. \quad (2.32)$$

It can be shown that $0 \leq \ell_+ \leq \ell_- \leq (1-\beta^2)^{-1/2}$.

The expression $1-\beta^2\epsilon$ can be rewritten as

$$1-\beta^2\epsilon = (1-\beta^2) \left[\frac{\prod_{q=1}^{2N-2} (v - Z_q)}{\prod_{j=1}^N (v + U_j^*)(v - U_j)} \right], \quad (2.33)$$

where the factors in the numerator give the positions of the zeroes of $1-\beta^2\epsilon$, while the poles of ϵ are given by the U_j 's. With the exception of $i\ell_+$, all the zeroes occur in the lower half plane, as do the poles which are at

$$v = U_j = \begin{cases} -in_j + (\nu_j^2 - n_j^2)^{1/2} & \nu_j > n_j \\ -i[n_j - (\eta_j^2 - \nu_j^2)^{1/2}] & \nu_j \leq n_j \end{cases} \quad (2.34)$$

and

$$v = -U_j^* = \begin{cases} -in_j - (\nu_j^2 - n_j^2)^{1/2} & \nu_j > n_j \\ -i[n_j + (\eta_j^2 - \nu_j^2)^{1/2}] & \nu_j \leq n_j \end{cases} \quad (2.33)$$

The complex values of Z_j are obtained numerically when N is greater than one.

For each pole U_j in the fourth quadrant, there will be an associated zero Z_j

such that $\lim_{\beta \rightarrow 0} Z_j = U_j$.

In Figure 1, the contour C_6 encloses the pair of points U_j and Z_j . Since $E_1(Z)$ is defined with a branch cut from zero to $-\infty$, a cut between Z_j and U_j has been introduced in Figure 1 such that C_6 does not cross the cut. The function $E_1(Z)$ on either side of the cut differs by $2\pi i$, where Z is defined by (2.27). Using this result in (2.21), the contour integral $I(C_6)$ can be expressed as

$$I(C_6) = 2\pi i \int_{Z_j}^{U_j} dv \frac{1}{\epsilon} (1-\beta^2\epsilon) e^{Av^2(1-\beta^2\epsilon)} [e^{-iB_1 v} + e^{-iB_2 v}] \quad (2.34)$$

along a path

$$v = Z_j + re^{i\delta}, \quad (2.35)$$

where

$$\delta = \tan^{-1} \left[\frac{-\text{Im}(U_j - Z_j)}{\text{Re}(U_j - Z_j)} \right]. \quad (2.36)$$

For each pair (Z_j, U_j) in the fourth quadrant there will be a contribution like $I(C_6)$.

If the dielectric function contains conduction electrons, there is a pole of ϵ on the imaginary axis at $v = -2i\eta_c$, where $2\eta_c \omega_p$ is the collision frequency or the plasmon width, as appropriate. In this case $Z < 0$ for $\gamma \leq 2\eta_c$ (see Equations (2.27) and (2.30)) and again

$$E_1(Z) = -Ei(|Z|) + i\pi, \quad y \leq 2\eta_c; \quad (2.37)$$

therefore,

$$I(C_7) = \pi \int_0^{2\eta_c} dy \frac{1}{\epsilon(-iy)} (1-\beta^2\epsilon(-iy))c^{-Ay^2(1-\beta^2\epsilon)} [e^{-B_1 y} + e^{-B_2 y}] \quad (2.38)$$

Note, for the case in which ϵ contains conduction electrons $\lim_{\beta \rightarrow 0} \epsilon = 2\eta_c$.

The contribution to (2.25) from the residues R_j of the poles of ϵ^{-1} at $v = \alpha_j$ (see (2.19)) can be written by inspection of Equation (2.21): if $\lambda_j > \eta_j$,

$$R_j = \frac{-f_j}{\alpha_j - \beta_j} e^{A\alpha_j^2} E_1(A\alpha_j^2) [e^{-iB_1 \alpha_j} + e^{-iB_2 \alpha_j}] \quad (2.39)$$

if $\lambda_j < \eta_j$,

$$R_j = \frac{-f_j}{2(\alpha_j - \beta_j)} \left\{ \begin{array}{l} e^{-A|\beta_j|^2} Ei(A|\beta_j|^2) [e^{-B_1 |\beta_j|} + e^{-B_2 |\beta_j|}] \\ -e^{-A|\alpha_j|^2} Ei(A|\alpha_j|^2) [e^{-B_1 |\alpha_j|} + e^{-B_2 |\alpha_j|}] \end{array} \right\} \quad (2.40)$$

In the latter case the poles lie on the imaginary axis (Equation 2.18b).

All of the quantities required to evaluate $I(C_1)$ and $I(C_8)$ appearing in W_B , Equation (2.26), have now been specified. $I(C_3)$, $I(C_5)$, $I(C_6)$ and $I(C_7)$ have been expressed as integrals which must be done numerically. In the nonrelativistic regime, an analytic approximation to W_B has been given previously,²¹ which agrees well with the corresponding numerically integrated result.

CHAPTER 3

NUMERICAL RESULTS FOR A RELATIVISTIC BEAM IN NITROGEN

The expression for W_B , Equation (2.26) has been evaluated numerically for the case of an electron beam pulse with an energy of 50.59 MeV ($\beta=0.99995$, $\gamma = 100.0$). The Gaussian radial profile parameter b_0 of Equation (2.9) was taken to be 0.1 cm and the beam density n_B was $6.623 \times 10^{13} \text{ cm}^{-3}$, which corresponds to a total current of 10 KA, or a current density of $3.18 \times 10^5 \text{ A/cm}^2$. The pulse length was 1 meter.

The medium is characterized by the dielectric function $\epsilon(\nu)$ with the parameters discussed in connection with Equations (2.15)-(2.17). Table I contains the values used in these expressions for $\epsilon(\nu)$ and $\epsilon^{-1}(\nu)$. The first three eigenfrequencies were taken from Reference 25. A more recent set has been given by Sternheimer and Peierls,²⁶ but the ones of Reference 25 are adequate for the present exploratory purpose. The K-shell line width was obtained from the compilation of widths made by Krause,²⁷ while the L_1 and L_2 widths were estimated from the formula for collisional line widths of Weisskopf as applied in Reference 28:

$$\hbar n_j = \frac{f_j}{8} \frac{(\hbar \omega_p)^2}{\hbar \omega_j} \quad [\text{eV}] \quad (3.1)$$

or

$$n_j = \frac{f_j}{8\nu_j}, \text{ units of } \omega_p. \quad (3.2)$$

TABLE 1. INPUT PARAMETERS TO CHARACTERIZE THE N₂ MEDIUM

See Equation (2.15) for definitions. The frequencies ν_j and n_j are in units of ω_p , where $\hbar\omega_p = 0.7208$ ev. The gas density is 1.1652×10^{-3} g/cm³. The parameter $\rho = 1.23$, see Equations (2.16) and (2.17).

j	f_j	ν_j	n_j
1	0.2587	572.4	4.9×10^{-2}
2	0.2587	66.1	4.4×10^{-4}
3	0.4286	43.4	1.0×10^{-3}
4	2.659×10^{-5}	0.0	3.63×10^{-3}

The value for f_4 was obtained by assuming that the N_2 medium was weakly ionized and had a free electron density of $n_e = 10^{16} \text{ cm}^{-3}$, corresponding to $KT \approx 0.7 \text{ eV}$. The parameter η_4 , in units of ω_p , is half the collision frequency ν_c , which can be obtained from the momentum transfer cross section,²⁹ $\sigma_m = 1.1 \times 10^{-15}$:

$$\nu_c \approx n \sigma_m \left(\frac{KT}{m} \right)^{1/2} = 1.0 \times 10^{12} \text{ sec}^{-1}, \quad (3.3)$$

where n is the gas density (see Table I).

According to the discussion below Equation (2.16),

$$l_4 = f_4^{1/2} = 5.156 \times 10^{-3}, \quad (3.4)$$

which corresponds to a plasma frequency of

$$\hbar\omega_4 = l_4 \hbar\omega_p = 3.716 \times 10^{-3} \text{ eV} \quad (3.5)$$

for the free electron component. Note that the ratio

$$\eta_4 / l_4 \approx 0.7, \quad (3.6)$$

so that the life time is of the order of the period of oscillation for this choice of parameters.

Figure 2 illustrates the results of the calculation of W_B , the beam-density effect on ionization energy loss for the particular set of parameters discussed above. The ratio of the beam to the single particle term, W_B/S , [see Equations (2.3) and (2.7)] is plotted versus the distance from the beam-front in centimeters. The curves shown are for a particle on the beam axis. The single-particle energy loss S (Equation (2.3)) was calculated using Sternheimer's method,²⁴ with the result that $S=2.48 \text{ MeV/g-cm}^{-2}$. The curves are symmetric with respect to the midpoint of the pulse at 50 cm. The solid curve was generated using the parameter values given in Table 1 with $n_e = 10^{16} \text{ cm}^{-3}$, while the dashed curve results when $n_e = 10^{17} \text{ cm}^{-3}$ and the dash-dot curve was obtained with $n_e = 10^{15} \text{ cm}^{-3}$. As above, n_e is the number of free electrons assumed to be present in the medium through which the pulse passes as it undergoes energy loss.

All three curves exhibit a large beam-density effect within the first millimeter from the beam front. At the midpoint of the pulse the three cases yield a ratio W_B/S of between one and two, which is still quite significant. The oscillatory behavior which occurs when $n_e = 10^{17} \text{ cm}^{-3}$ comes from the residues of the poles of ϵ^{-1} given by (2.39). The residue terms decay exponentially and begin to be dominated by the nonresonant terms at about 0.05 cm from the beam front. When $n_e = 10^{16}$ and 10^{15} cm^{-3} , the nonresonant contribution dominates the resonant part and the oscillatory behavior disappears.

For a particle at the beam front, $L_2 = 0$ and L_1 is equal to the pulse length, Equation (2.9). For a semi-infinite pulse, $L_1 \rightarrow \infty$, then if $L_2 = 0$ one obtains $W_B = 0$ (see Equation (2.14)). Even for the one meter pulse studied, $W_B/S \sim 10^{-1}$ at $L_2 = 0$, $L_1 = 1\text{m}$. This behavior provides a useful check on

E = 50 MeV
I = 10 KA
b₀ = 1 mm
L = 1 m
P = 1 Atm

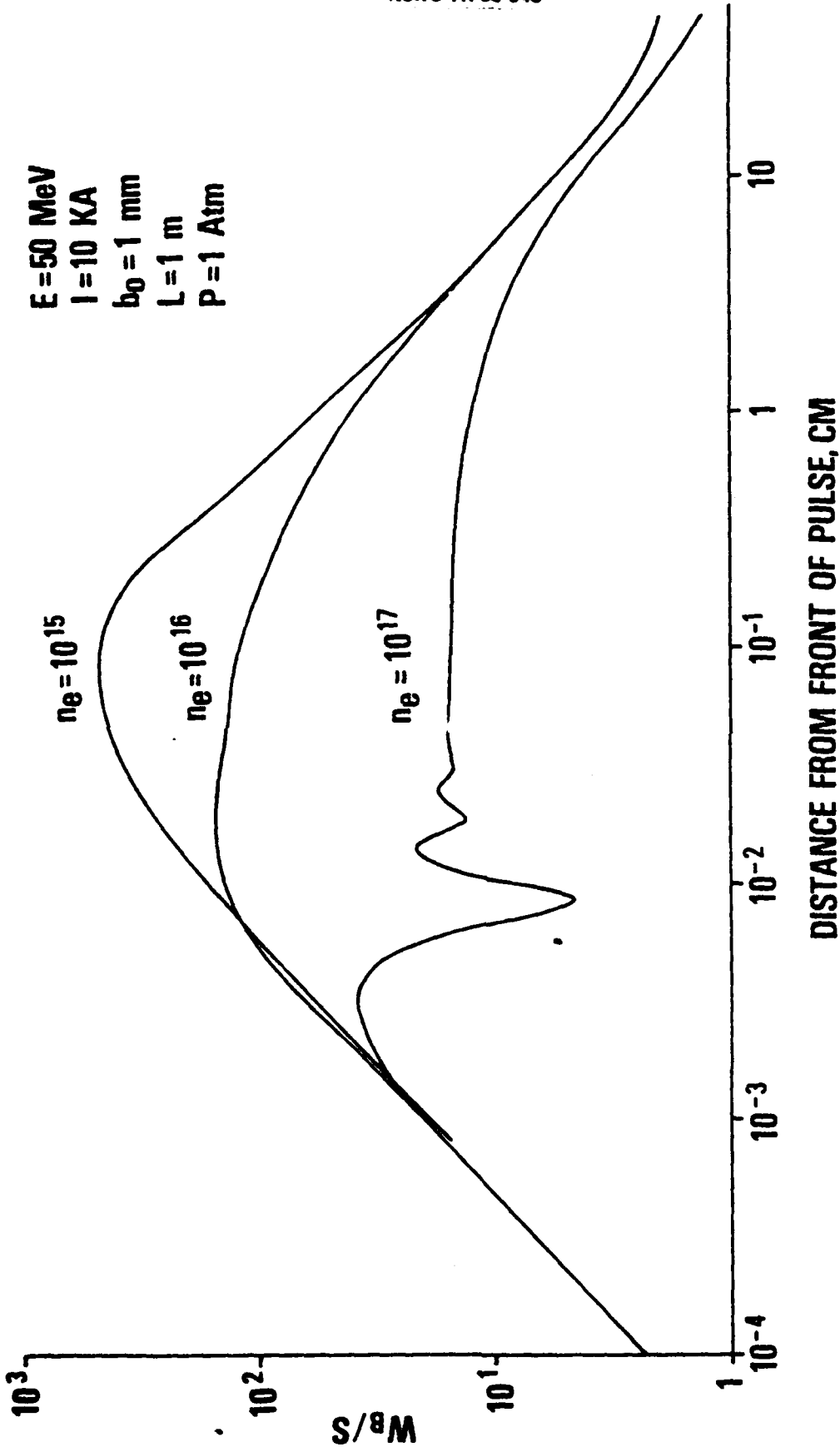


FIGURE 2. THE RATIO OF THE BEAM-DENSITY ENERGY LOSS TO THE SINGLE PARTICLE ENERGY LOSS, W_B/S

the numerical integrations, since the nonresonant terms calculated numerically must cancel exactly the analytical resonant terms at $L_2=0$ if $L_1=\infty$. This test was particularly useful in checking the case of $n_e=10^{15} \text{ cm}^{-3}$ since then $\eta_4 > k_4$ and the poles of $\epsilon^{-1}(\nu)$ at $\nu=\alpha_4$ and $\nu=\beta_4$ (see Equation 2.18b) lie on the imaginary axis. Then a principal value integral is required in order to evaluate $I(C_7)$, Equation (2.38), and the results are very sensitive to the numerical procedure used.

The results obtained for the individual contours of Figure 1 showed that the contributions from $I(C_3)$, $I(C_5)$, and $I(C_6)$ were negligible in this example. $I(C_7)$, however, resulted in the large beam-density contributions illustrated in Figure 2. When $\beta \ll 1$, $k_+ \rightarrow 0$ and $k_- \rightarrow 2\eta_4$ and there will be a small contribution from $I(C_3)$; also as $\beta \rightarrow 0$ $Z_j \rightarrow U_j$ and $I(C_6) \rightarrow 0$. It should be pointed out that the parameters used to model the dielectric function $\epsilon(\nu)$ given in Table 1 are based on the ionization potentials of the subshells of nitrogen and are not suitable for the investigation of Cerenkov radiation by beams; therefore, one does not expect to obtain any beam-density effect on Cerenkov radiation in the present example. By a suitable modification²⁸ of $\epsilon(\nu)$, the Cerenkov part of energy loss can easily be incorporated into this treatment.

The contributions to W_B from the contour integrals of Figure 1 all contain both longitudinal and transverse field components. The transverse components come from the singularities associated with $E_1(A\nu^2(1-\beta^2\epsilon))$, Equation (2.21), as $1-\beta^2\epsilon \rightarrow 0$ and $\epsilon \rightarrow \infty$. In the limit $\beta \rightarrow 0$ only longitudinal contributions remain. In Reference 21 it was shown that the longitudinal contribution from the contour

along the imaginary axis was of a long-range, dipole-like form for the cooperative loss between two particles. It is this long range, nonresonant contribution which is dominant in the present calculation. The resonant part, coming from the poles of $\epsilon^{-1}(\nu)$ Equation (2.39) is purely longitudinal and is a relatively short ranged term.

CHAPTER 4
DISCUSSION

The evaluation of W_B , Equation (2.26), and the results of the beam-density effect calculation presented in Chapter 3 contain no approximation other than those implicit in the models chosen to represent the medium and the beam. The medium was characterized by a dielectric function based on the assumption of linear response to the local \vec{E} -field. The validity of this assumption may be questionable near the beam-front where the fields have large, rapid variations. The derivation of Equation (2.26) was based on a spacially non-dispersive dielectric function, but a minimum impact parameter cut off was used (see Equation (2.1)) to separate the region of distant collisions with small momentum transfers from the region of high momentum collisions. This procedure has been found to yield good agreement with two-particle vicinage function calculations using a simple momentum dependent dielectric function in the nonrelativistic regime (see References 9-12 and 19). After integration over the beam, the effect of a non-zero minimum impact parameter was negligible.

The medium was assumed to remain in its initial state during the interaction with the pulse. Therefore, the increase in medium conductivity produced by the deposited beam energy has not been incorporated in a self-consistent way with the energy-deposition calculation. The variation of n_e , the number of free electrons per cm^3 , was given in Figure 2 to illustrate roughly the possible effect of changes in conductivity. This first calculation

is intended primarily to explore the basic properties and magnitude of the beam-density effect and its relation to other phenomena rather than to be a definitive self-consistent treatment.

The beam pulse was modeled by a charged fluid with a step function head and tail and a Gaussian radial profile. The abrupt rise of current in this model is somewhat unrealistic. For a more gradual current rise and fall, the values of W_B near the beam front and tail may be considerably less than those found in the present calculation. The question of how well a fluid model simulates the more realistic case of a system of discrete beam particles which are distributed according to an appropriate correlation function requires further consideration also. Note that the starting point of the present treatment was two discrete beam particles separated by an arbitrary position vector.

Setting aside the caveats discussed above, Figure 2 shows that the particles in a 1 meter pulse experience energy loss at a rate which is greater than twice that of a single-particle. Near the head and tail, the loss rate for a 50 MeV, 10KA beam of 0.1 cm radius can range over one or two orders of magnitude, depending on the ionization state of nitrogen at 1 atmosphere. Longer pulses will have a smaller proportion of their electrons which experience a large beam-density loss. The magnitude of this loss per particle is directly proportional to the current density. Further studies of the dependence of W_B on medium and beam parameters are underway.

In order to relate the beam-density effect as presented in the present paper to the single-particle ionization energy loss, and at the same time to the phenomena of ohmic loss and return currents^{14,18} in plasmas, a brief discussion

of the various approaches to energy loss will be useful. The ionization energy loss of a single particle may be considered from any of three equivalent points of view: a) the work done on the medium by the particle's \vec{E} -field, the Bohr viewpoint,²² b) the work done on the particle by the field induced in the medium, the Landau viewpoint, and c) the Poynting flux through the surface of a cylinder surrounding the particle's trajectory, the Fermi viewpoint.²² The equivalence of these three approaches is well known and can be proven using the Poynting theorem. In the case of beams of particles, a similar equivalence has been derived in Reference 19. There it was shown that the rate of change of mechanical energy of a beam caused by the induced field of the medium is

$$\frac{dE_M}{dt} = \int \vec{J} \cdot (\vec{E} - \vec{D}) d^3x = -4\pi \sum_{i=1}^n Z_i e \vec{v}_i \cdot \vec{P}, \quad (4.1)$$

where \vec{P} is the total induced polarization field caused by all beam particles; $4\pi\vec{P} = \vec{D} - \vec{E}$; and the beam current is $\vec{J} = \sum Z_i e \vec{v}_i \delta(\vec{r} - \vec{v}_i t - \vec{R}_i)$. This expression excludes internal transformation of beam field energy to beam mechanical energy, which would occur even in the absence of a medium. In terms of the induced polarization field associated with each beam particle, $\vec{P} = \sum_{j=1}^n \vec{P}_j$ and one may write

$$\frac{dE_M}{dt} = -4\pi \sum_{i=1}^n Z_i e \vec{v}_i \cdot \sum_{j=1}^n \vec{P}_j. \quad (4.2)$$

In this expression the terms with $i=j$ are the usual single-particle terms and those with $i \neq j$ are the cooperative beam terms. For the i th particle, one has

$$\frac{dE_{Mi}}{dt} = -4\pi Z_i e \vec{v}_i \cdot \vec{P}_i - 4\pi Z_i e \vec{v}_i \cdot \sum_{j=1}^n \vec{P}_j, \quad j \neq i. \quad (4.3)$$

If all the beam particles are assumed to have equal velocities, v , then $v^{-1} dE_{Mi}/dt$ corresponds to Equation (2.7).

Focusing attention on the beam, one sees that (4.1) or (4.3) has the general form of ohmic loss caused by the interaction of the induced medium field with the beam. This is essentially the Landau viewpoint discussed above. If, instead, the response of the medium to the beam's fields is considered, then one has the Bohr viewpoint. Since the dielectric function used in the present calculation includes the contribution from the conduction electrons, the Bohr viewpoint will encompass the phenomenon of the return current induced by the beam, as well as the polarization currents of the bound electrons.¹⁴ These currents are just $d\vec{P}/dt$.

In the present calculation it was found that the dominant beam-density effect comes from the nonresonant, low frequency contribution to the frequency integral of W_B . This part of the effect may be identified with ohmic loss in a plasma. However, both the resonant and nonresonant terms are required in order to obtain the proper behavior of W_B at the beam front and at a point infinitely far from the head or tail of an infinite beam.²¹ The relation of $W(z,b)$, Equation (2.1), to the nonrelativistic two-particle vicinage functions^{7,19} has already been discussed in Chapter 2. Formally, $W(z,b)$ also contains the Fermi density effect,²⁰ including the Čerenkov loss term. The integral of $W(z,b)$ over a beam further incorporates the ohmic loss term along with these one- and two-particle energy loss phenomena. Therefore, from a formal point of view the present treatment includes all the various aspects of collisional energy loss by charged particle beams in a unified way.

REFERENCES

1. Toepfer, Alan J., "Particle Beam Fusion," Advances in Electronics and Electron Physics, Vol. 53, 1980, p.1.
2. Imasaki, K., et al., "Evidence of Anomalous Interaction Between a Relativistic Electron Beam and Solid Target," Physical Review Letters, Vol. 43, 1979, p. 1937.
3. Imasaki, K., et al., "Energy Absorption and Transport in Layered Targets Irradiated by a Relativistic Electron Beam," Applied Physics Letters, Vol. 37, No. 6, 1980, p. 533.
4. Young, F. C. et al., "Measurements of Enhanced Stopping of 1-MeV Deuterons in Target-Ablation Plasmas," Physical Review Letters, Vol. 49, 1982, p. 549.
5. Kiselev, V. A., et al., "Interaction of a Relativistic Monochromatic Electron Beam with Plasma Produced in the Atmosphere," Soviet Physics JETP Letters, Vol. 29, No. 12, 1979, p. 700.
6. McCorkle, R. A., and Iafrate, G. J., "Beam-Density Effect on the Stopping of Fast Charged Particles in Matter," Physical Review Letters, Vol. 39, No. 20, 1977, p. 1263.

REFERENCES (Cont.)

7. Brandt, Werner, Ratkowski, Anthony, and Ritchie, R. H., "Energy Loss of Swift Proton Clusters in Solids," Physical Review Letters, Vol. 33, No. 22, 1974, p. 1325.
8. Brandt, Werner and Ritchie, R. H., "Penetration of Swift Ion Clusters Through Solids," Nuclear Instruments and Methods, Vol. 132, 1976, p. 43.
9. Basbas, George, and Ritchie, R. H., "Vicinage Effects in Ion-Cluster Collisions with Condensed Matter and with Single Atoms," Physical Review A, Vol. 25, No. 4, 1982, p. 1943.
10. Neelavathi, V. N., Ritchie, R. H., and Brandt, Werner, "Bound Electron States in the Wake of Swift Ions in Solids," Physical Review Letters, Vol. 33, No. 5, 1974, p. 302.
11. Ritchie, R. H., Brandt, Werner, and Echenique, P. M., "Wake Potential of Swift Ions in Solids," Physical Review B, Vol. 14, No. 11, 1976, p. 4808.
12. Mazarro, A., Echenique, P. M., and Ritchie, R. H., "Charge-Particle Wake in the Random-Phase Approximation," Physical Review B, Vol. 27, No. 7, 1983, p. 4117.
13. McCorkle, R. A., and Cox, J. L. Jr., "Beam-Plasma Electrodynamics," Physics Letters, Vol. 83A, No. 9.

REFERENCES (Cont.)

14. Roberts, T. G., and Bennet, W. H., "The Pinch Effect in Pulsed Streams at Relativistic Energies," Plasma Physics, Vol. 10, 1968, p. 381.
15. Cox, James L., Jr. and Bennett, Willard H., "Reverse Current Induced by Injection of a Relativistic Electron Beam into a Pinched Plasma," Physics of Fluids, Vol. 13, No. 1, 1970, p. 182.
16. Hammer, D. A., and Rostocker, N., "Propagation of High Current Relativistic Electron Beams," Physics of Fluids, Vol 13, No. 7, 1970, p. 1831.
17. Lovelace, R. V., and Sudan, R. N., "Plasma Heating by High-Current Relativistic Electron Beams," Physical Review Letters, Vol. 27, No. 19, 1971, p. 1256.
18. Wallis, G. et al., "Injection of High-Current Relativistic Electron Beams into Plasma," Soviet Physics-Uspekhi, Vol. 17, No. 4, 1975, p. 492.
19. Rule, D. W., and Cha, M. H., "Collective Effects in Energy Loss by Relativistic Clusters of Charged Particles," Physical Review A, Vol. 24, No. 1, 1981, p. 55.
20. Rule, D. W., "Collective Effect in Energy Deposition by Beams of Relativistic Charged Particles," in High-Power Beams 81, Proceedings of the Fourth International Topical Conference on High-Power Electron and Ion-Beam Research and Technology-Palaiseau, 29 June 1981, pp. 481-488.

REFERENCES (Cont.)

21. Rule, D. W., and Crawford, O. H., The Nature of the Beam-Density Effect on Energy Loss by Nonrelativistic Charged Particle Beams, NSWC TR 83-346, June 1983.
22. Jackson, J. D., Classical Electrodynamics, 2nd ed. (John Wiley and Sons, Inc., New York, 1975) pp. 618-653.
23. Gradshteyn, I. S., and Ryzhik, I. M., Tables of Integrals, Series, and Products (Academic Press, New York, 1980), p. 717.
24. Sternheimer, R. M., "The Density Effect for the Ionization Loss in Various Materials," Physical Review, Vol. 88, No. 4, 1952, p. 851.
25. Sternheimer, R. M., "Density Effect for the Ionization Loss in Various Materials," Physical Review, Vol. 103, No. 3, 1956, p. 511.
26. Sternheimer, R. M., and Peierls, R. F., "General Expression for the Density Effect for the Ionization Loss of Charged Particles," Physical Review B, Vol. 3, No. 11, 1971, p. 3681.
27. Krause, M. O., "Atomic Radiative and Radiationless Yields for K and L Shells," Journal of Physical and Chemical Reference Data, Vol. 8, 1979, p. 307.
28. Sternheimer, R. M., "The Energy Loss of a Fast Charged Particle by Cerenkov Radiation," Physical Review, Vol. 91, No. 2, 1953, p. 256.

REFERENCES (Cont.)

29. Itikawa, Yukikazu, "Momentum Transfer Cross Sections for Electron Collisions with Atoms and Molecules," Atomic Data and Nuclear Data Tables, Vol. 14, No. 1, 1974, p. 1.

30. Landau, L. M., and Lifshitz, E. M., Electrodynamics of Continuous Media (Addison-Wesley Publishing Co., Inc., Reading, MA, 1960) pp. 344-359.

DISTRIBUTION

<u>Copies</u>	<u>Copies</u>
Commanding Officer Naval Research Lab Attn: Code 4700 (Dr. W.A. Ali) 1 Code 6650 (Dr. J.B. Aviles, Jr.) 1 Code 4770 (Dr. Richard Fernsler) 1 (Dr. S. Goldstein) 1 Code 4763 (Dr. Robert Greig) 1 Code 4790 (Dr. M. Lampe) 1 Code 4740 (Dr. C. W. Roberson) 1 Code 6654 (Dr. Alex Stolovy) 1 (Dr. F. C. Young) 1 Washington, D. C. 20375	Director, National Bureau of Standards Attn: (Dr. Mark Wilson) 1 Gaithersburg, MD 20760 Physical Review Letters Attn: (Dr. George Basbas) 1 Box 1000 Ridge, NY 11961 Lawrence Livermore Natl. Lab. Attn: (Dr. R. Briggs) 1 P.O. Box 808 Livermore, CA 94550 Lawrence Livermore Natl. Lab. Attn: (Dr. Thomas Fessenden) 1 (Dr. Simon S. Yu) 1 L321 University of California Livermore, CA 94550 La jolla Institute Attn: (Dr. K. Brueckner) 1 P.O. Box 1434 La Jolla, CA 92038 Oak Ridge National Lab. Attn: Chemistry Division (Dr. Oakley Crawford) 1 Health & Safety Res. Div. (Dr. Rufus H. Ritchie) 1 Oak Ridge, TN 37830 Los Alamos National Laboratory Attn: (Dr. Harold Dogliani) 1 Mail Sta. H818, P.O. Box 1663 Los Alamos, NM 87545 Physical Dynamics, Inc. Attn: (Dr. George Gillespie) 1 P. O. Box 1883 La Jolla, CA 92038 Laboratory of Plasma Studies Attn: (Prof. D. Hammer) 1 Cornell University Ithaca, NY 14850
Commander, Naval Sea Systems Command Attn: (D.L. Merritt) 1 11N08 NC1 Washington, D. C. 20362	
Office of Naval Research Attn: (Dr. B. R. Junker) 1 800 N. Quincy St. Arlington, VA 22217	
Commander, Harry Diamond Lab Attn: (Dr. S. Graybill) 1 2800 Powder Mill Road Adelphi, MD 20783	
U.S. Army Ballistic Research Lab. Attn: (Dr. D. Eccleshall) 1 Aberdeen Proving Ground, MD 21005	
4FWAL-MLPJ Attn: (Dr. Peter L. Land) 1 Bldg. 451 Wright-Patterson AFB, OH 45433	
Director, Nat'l. Bureau of Standards Center for Radiation Research Attn: (Dr. M.J. Berger) 1 (Dr. S. M. Seltzer) 1 Washington, D. C. 20234	

DISTRIBUTION (Cont.)

<u>Copies</u>	<u>Copies</u>
Argonne National Laboratory Attn: (Dr. Mitio Inokuti) 1 Building 203 9700 South Cass Avenue Argonne, ILL 60439	Dartmouth College Dept. of Physics Attn: (Dr. John E. Walsh) 1 Hanover, NH 03755
Science Applications, Inc. Attn: (Dr. Robert Johnston) 1 5 Palo Alto Square Palo Alto, CA 94304	Defense Technical Information Center Cameron Station Alexandria, VA 22314 12
General Dynamics Corp. Materials Technology Div. Attn: (Dr. Frank L. Madarasz) 1 Mail Zone 44-68, P. O. Box 2507 Pomona, CA 91769	Internal Distribution
Sandia National Laboratories Attn: (Dr. E.J. McGuire) 1 Target Int. Theory Div.- 4247 (Dr. T. A. Mehlhorn) 1 Division 5246 (Dr. Bruce R. Miller) 1 Albuquerque, NM 87115	R 1 R04 1 R40 1 R401 1 R13 (J. Forbes) 1 R41 (P. W. Hesse) 1 R41 (R. Cawley) 1 R41 (M. H. Cha) 1 R41 (H. C. Chen) 1 R41 (R. Fiorito) 1 R41 (O. F. Goktepe) 1 R41 (H. S. Uhm) 1 R34 (DR. J. Sharma) 1 F 1 F34 (E. Nolting) 1 F04 (M. F. Rose) 1 E431 9 E432 3 E35 1
Thomas J. Watson Research Center IBM Attn: (Dr. Richard McCorkle) 1 Yorktown Heights, N. Y. 10598	
University of California Dept. of Physics Attn: (Prof. N. Rostoker) 1 Irvine, CA 92664	
Brookhaven National Laboratory Dept. of Physics Attn: (Dr. R.M. Sternheimer) 1 Upton, NY 11973	
Cornell University Lab. of Plasma Studies Attn: (Prof. R. Sudan) 1 Ithaca, NY 14850	

ED

88